Poloidal impurity asymmetry studies using the upgraded high field side edge CXRS diagnostic at ASDEX Upgrade

D.J Cruz-Zabala[1,2], E. Viezzer[1,2], M. Cavedon[3], P. Cano-Megias[4,2], U. Plank[3], R. Dux[3], J. Garcia-Lopez[1,2], M. Garcia-Munoz[1,2], M. Griener[3], R. M. McDermott[3], T. Pütterich[3] and ASDEX Upgrade Team[3]

[1] *Dept. of Atomic, Molecular and Nuclear Physics, University of Seville, Seville, Spain*

[2] *CNA (U. Sevilla, CSIC, J. de Andalucia), Seville, Spain*

[3] *Max-Planck-Institut für Plasmaphysik, Garching, Germany*

[4] *Dept. of Energy Engineering, University of Seville, Seville, Spain*

Introduction. Several studies have shown poloidal asymmetries when comparing impurity profiles at the low field side (LFS) and high field side (HFS) [1, 2, 3]. At ASDEX Upgrade, the inboard-outboard impurity density asymmetry can reach a factor of 3, while the temperature and the electrostatic potential are found to be flux functions [4]. Impurity profiles are normally measured using the charge exchange recombination spectroscopy (CXRS) technique. In order to study the impurity asymmetries in further detail, the high field side (HFS) edge CXRS diagnostic has been upgraded. This work will show the first study of asymmetries in impurity temperature, velocity and density using the upgraded system.

Experimental setup. The high field side CXRS system at the plasma edge of ASDEX Upgrade has been upgraded with a new gas valve [5] and a new poloidal optical head. This new valve injects thermal neutrals very localized at the edge of the plasma to induce charge exchange reactions. The light emitted due to the reactions is collected by the new poloidal and the already existing toroidal optical heads. The fast opening and closing (~ 2 ms) of the new piezoelectric valve allow for a better characterization of the background emission. Dedicated calibrations for different gases have been performed in order to determine the flowrate accurately. Moreover, the number of lines of sight (LOS) has been increased to improve the radial resolution. Figure 1 shows an overview of the upgraded system.

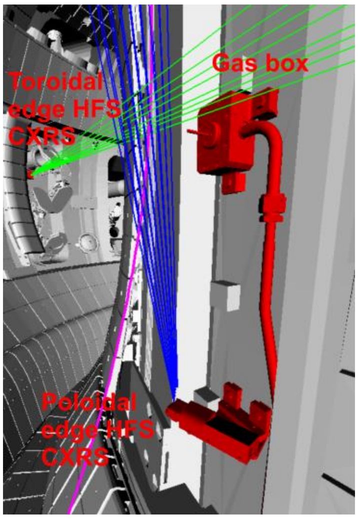

Figure 1. Scheme of the HFS CXRS system. Magenta line corresponds to the separatrix.

Experimental results. The experiments were carried out in H-mode plasmas with a plasma current of 1 MA and a toroidal magnetic field of 2.5 T. The time traces of NBI power, ECRH power, electron density, outer radial plasma position (Raus) and fuelling are shown in figure 2. Apart from the upgraded system at the HFS, two more CXRS systems were measuring during these experiments at the LFS: a beam based CXRS system [6, 7] and a gas puff based CXRS system [8]. In order to maximize the capabilities of both LFS and HFS CXRS systems, a scan was done moving the outer radial plasma position (Raus). Initially the plasma was moved towards the outer wall (Raus ~ 2.16 m) in order to measure properly with the LFS systems. As shown in figure 2(c), during this phase, blips in the LFS valve were performed. At around 3.0 s, the plasma is moved to the inner wall (Raus ~ 2.10 m) in order to maximize the coverage of the HFS upgraded system. From 3.0 s to 5.0 s blips of 30 ms in the HFS valve were performed. This scan is repeated from 5.0 s onwards. Note that NBI source 3 blips are performed when the plasma is close to the outer wall as this source is needed for the beam based CXRS system. Constant nitrogen seeding was used to increase the signal level. Combining the measurements of the three systems, the possible asymmetries between LFS and HFS can be studied. Figure 3 shows a comparison of impurity temperature, poloidal velocity and toroidal velocity between LFS and HFS. The impurity profiles were aligned to the electron temperature profile. The electron temperature was shifted that it takes a value of 100 eV at the separatrix. In this case, only a 5 mm shift was applied in the LFS impurity profiles. Within the scattering of the HFS data, no asymmetries are observed in the impurity temperature even if no shift had been applied. The absence of asymmetries in

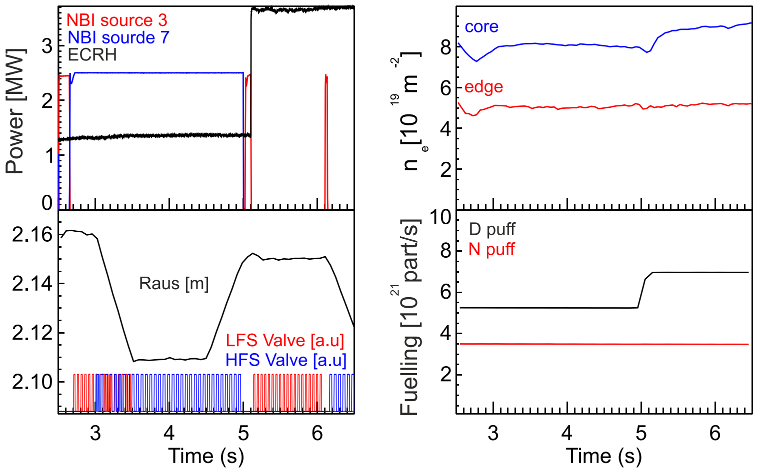

Figure 2. Power, electron density, Raus and fuelling time traces

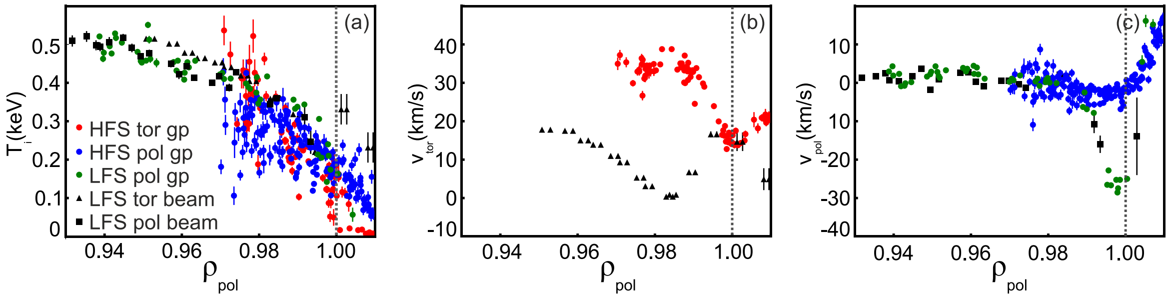

Figure 3. Impurity temperature (a), toroidal velocity (b) and poloidal velocity (c) profiles. Dash line corresponds to the separatrix.

the impurity temperature was expected from previous studies [2, 4]. The poloidal and toroidal velocities have different shapes when comparing LFS and HFS. While the toroidal velocity at the LFS presents a minimum close to $\rho_{\mathrm{pol}} = 0.98$, it has a maximum at the HFS at approximately the same position. They reach almost the same value when approaching the separatrix. Regarding the poloidal velocity, it has a clear minimum close to the separatrix at the LFS while it has a less prominent minimum in the HFS. The asymmetries in the flows can be explained by an excess of impurity density at the HFS [1, 2, 4]. Considering an impurity density asymmetry, the lowest order of divergence-free impurity velocity can be expressed as follows:

$$\overrightarrow{v_\alpha} = \omega_\alpha(\psi) R \overrightarrow{e_\phi} + \frac{k_\alpha(\psi)}{n_\alpha} B \overrightarrow{e_{||}}$$

where ψ is the poloidal magnetic flux, $\omega_\alpha(\psi)$ and $k_\alpha(\psi)$ are flux functions, R is the local major radius, $\overrightarrow{e_\phi}$ and $\overrightarrow{e_{||}}$ are the toroidal and parallel unit vectors, n_α is the impurity density and B is the magnetic field. Assuming that n_α is a flux function, $k_\alpha(\psi)$ would result in $k_\alpha(\psi) = \frac{v_{\theta,\alpha}}{B_\theta}$. Figure 3(c) shows that $v_{\theta,\alpha}^{\mathrm{HFS}} < v_{\theta,\alpha}^{\mathrm{LFS}}$ and knowing that $B_\theta^{\mathrm{HFS}} > B_\theta^{\mathrm{LFS}}$ it would mean that $k_\alpha(\psi)$ is not a flux function. This indicates that a poloidal impurity density asymmetry is present in the very edge of the plasma. Note that this expression is an approximation and terms related to sources and sinks are not included.

Impurity density calculation. In order to calculate the impurity density profile at the HFS, modelling of the neutral density is needed. In the case of thermal neutrals, the average impurity density at the intersection of LOS and gas puff can be calculated as $n_\alpha = 4\pi \frac{L_{\mathrm{CX}}^{\mathrm{ph}}(\lambda)}{\int_{\mathrm{LOS}} \langle \sigma_{\mathrm{n=2}} v \rangle n_{\mathrm{D,n=2}} dl}$, where $L_{\mathrm{CX}}^{\mathrm{ph}}(\lambda)$ is the experimental radiance, $n_{\mathrm{D,n=2}}$ is the neutral density with main quantum number $n = 2$ and $\langle \sigma_{\mathrm{n=2}} v \rangle$ is the effective reaction rate. Note that the integral is along a line of sight (LOS). In the case of thermal neutrals, the contribution of neutrals in the $n = 2$ is dominant [3]. During this work, the FIDASIM code [9, 10] has been used to model the gas puff penetration. For this purpose, a new model has been implemented in the code that simulates a gas puff. This module launches neutrals from the HFS with thermal energy. For testing the model, D atoms are considered instead of D_2 molecules. A more realistic model should include molecular effects. The implementation of the geometry of the gas cloud in the model has been compared and validated with the experimental one determined in a glow discharge in a vacuum chamber. This geometry consists in a cone around the injection direction with an opening angle of 20°. The calibration of the flowrate of the valve allows us to determine the real flowrate accurately, which is used as an input for the new gas puff model. Figure 4(a) shows a poloidal view of the first generation of gas puff neutrals when the plasma was close to the inner wall. Knowing the neutral distribution and the experimental radiance, the impurity density profile can be calculated. Figure 4(b) shows the impurity density profile at the HFS calculated using the neutrals modelled with FIDASIM. Each point on this plot corresponds to a LOS.

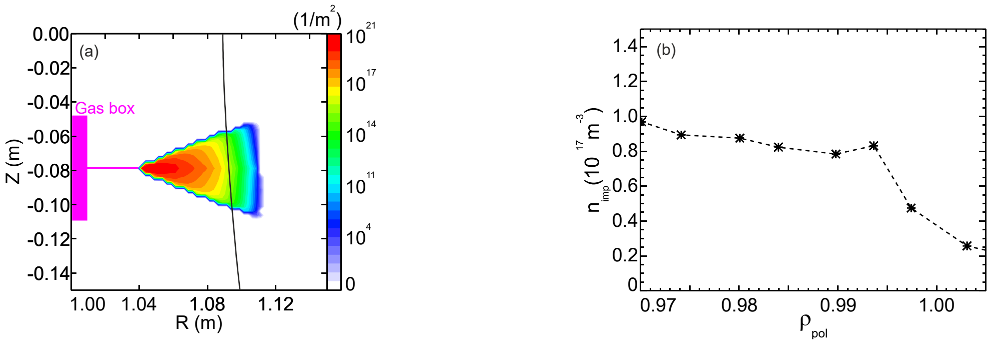

Figure 4. Poloidal view of the gas puff cloud (a). $\boldsymbol{n_\alpha}$ at the HFS calculated modelling thermal neutrals with FIDASIM (b).

Conclusions. The first study of poloidal asymmetries using the upgraded HFS CXRS system at ASDEX Upgrade is presented. While the temperature is a flux function, poloidal and toroidal velocities show asymmetries that can be explained by an excess of impurity density at the HFS. The impurity density profile at the HFS has been calculated using a new model included in FIDASIM that simulates gas puff neutrals.

Acknowledgements. This work received funding from the VI Plan Propio de Investigación de la Universidad de Sevilla (PPITUS 2017). This work has been carried out within the framework of the EUROfusion Consortium and has received funding from the Euratom research and training programme 2014-2018 and 2019-2020 under grant agreement No 633053. The views and opinions expressed herein do not necessarily reflect those of the European Commission.

References

[1] K.D Marr et al. Plasma Physics and Controlled Fusion, 52:055010, 2010.

[2] T. Pütterich et al. Nuclear Fusion, 52:083013, 2012.

[3] R.M. Churchill et al. Nuclear Fusion, 53:122002, 2013.

[4] E. Viezzer et al. Nuclear Fusion, 55:123002, 2015.

[5] M. Griener et al. Review of Scientific Instruments, 88:033509, 2017.

[6] E. Viezzer et al. Review of Scientific Instruments, 83:103501, 2012.

[7] M. Cavedon et al. Review of Scientific Instruments, 88:043103, 2017.

[8]. U. Plank, EPS, 2019

[9] W. W. Heidbrink et al. Communications in Computational Physics 10:716, 2011.

[10] B. Geiger, PhD thesis, LMU München (2013).